HscA and HscB Stimulate [2Fe-2S] Cluster Transfer from IscU to Apoferredoxin in an ATP-Dependent Reaction†

Kala Chandramouli and Michael K. Johnson*

Department of Chemistry and Center for Metalloenzyme Studies, University of Georgia, Athens, Georgia 30602

Received June 21, 2006; Revised Manuscript Received July 24, 2006

ABSTRACT: The role of the *Azotobacter vinelandii* HscA/HscB cochaperone system in ISC-mediated iron−sulfur cluster biogenesis has been investigated in vitro by using CD and EPR spectrometry to monitor the effect of HscA, HscB, MgATP, and MgADP on the time course of cluster transfer from [2Fe-2S]IscU to apo-Isc ferredoxin. CD spectra indicate that both HscB and HscA interact with [2Fe-2S]IscU and the rate of cluster transfer was stimulated more than 20-fold in the presence stoichiometric HscA and HscB and excess MgATP. No stimulation was observed in the absence of either HscB or MgATP, and cluster transfer was found to be an ATP-dependent reaction based on concomitant phosphate production and the enhanced rates of cluster transfer in the presence of KCl which is known to stimulate HscA ATPase activity. The results demonstrate a role of the ISC HscA/HscB cochaperone system in facilitating efficient [2Fe-2S] cluster transfer from the IscU scaffold protein to acceptor proteins and that [2Fe-2S] cluster transfer from IscU is an ATP-dependent process. The data are consistent with the proposed regulation of the HscA ATPase cycle by HscB and IscU [Silberg, J. J., Tapley, T. L., Hoff, K. G., and Vickery, L. E. (2004) *J. Biol. Chem. 279*, 53924−53931], and mechanistic proposals for coupling of the HscA ATPase cycle with cluster transfer from [2Fe-2S]IscU to apo-IscFdx are discussed.

Iron−sulfur cluster biogenesis proteins in bacteria are commonly encoded by a highly conserved *isc* (*i*ron−*s*ulfur *c*luster) gene cluster, *iscRSUA-hscBA-fdx* (*1*). Moreover, with the exception of the regulatory protein IscR, homologues of each of these proteins have been shown to be involved in Fe-S cluster biogenesis in eukaryotic organisms (*2*). Extensive biochemical and genetic studies have established well-defined roles for IscS and IscU, but specific roles for the IscA, HscA,[1] HscB, and Fdx proteins remain elusive. IscS is a cysteine desulfurase that catalyzes the conversion of cysteine to alanine (*3*, *4*) and thereby provides the inorganic sulfur for assembly of [2Fe-2S] or [4Fe-4S] clusters on the IscU scaffold protein (*5*). In vitro studies have shown that IscA has the ability to function as either an alternative scaffold for IscS-mediated cluster assembly of [2Fe-2S] or [4Fe-4S] clusters (*6*, *7*) or as a specific Fe donor for cluster assembly on IscU (*8*), but the physiologically relevant role has yet to be determined. Likewise, the specific redox role of the Isc $[2Fe\text{-}2S]^{2+,+}$ Fdx (*f*erre*dox*in) in IscS-mediated cluster assembly has yet to be identified, with reduction of S^0 to S^{2-}, oxidation of Fe^{2+} to Fe^{3+} in the assembly of $[2Fe\text{-}2S]^{2+}$ clusters, and reductive coupling of two $[2Fe\text{-}2S]^{2+}$ clusters on IscU to yield one $[4Fe\text{-}4S]^{2+}$ cluster as the most likely candidates (*5*, *9*).

In vivo gene knockout studies have demonstrated that both HscA (*h*eat *s*hock *c*ognate 66 kDa; Hsc66) and HscB (*h*eat *s*hock *c*ognate 20 kDa; Hsc20), and their eukaryotic homologues, Ssq1 and Jac1, have crucial roles in the maturation of Fe-S proteins in both prokaryotic and eukaryotic organisms (*10*−*14*). HscA and HscB function together as a nucleotide-dependent molecular chaperone system that is specific for IscU (*15*−*17*). HscA is a specialized member of the ubiquitous 70 kDa heat shock protein (Hsp70 or DnaK) family of molecular chaperones that facilitate protein folding, (dis)assembly, and transport via nucleotide-dependent binding to unfolded, misfolded, or unstable polypeptides in order to prevent nonspecific aggregation processes (*18*). The biochemical and structural properties of HscA, including distinct peptide- and nucleotide-binding domains, low intrinsic ATPase activity, and nucleotide-dependent peptide binding, are similar to those of Hsp70s (*17*, *19*, *20*), but HscA has distinct substrate and cochaperone specificity (*15*, *16*, *21*, *22*). HscA is able to interact with either the cluster-loaded or apo forms of IscU (*21*) and selectively binds to a highly conserved LPPVK motif (*16*, *22*) located adjacent to the putative solvent-exposed cluster binding site on IscU (*23*, *24*). Interestingly, recent structural characterization of the HscA substrate-binding domain complexed with a small peptide containing the LPPVK motif revealed that the peptide binds with the opposite orientation to that observed in DnaK peptide complexes (*20*). HscB is a specialized member of the J-type cochaperone (Hsp20 or DnaJ) family that escorts the IscU substrate to HscA and enhances the HscA−IscU interaction by coupling ATP binding and hydrolysis with conformational changes involving tense (T) and relaxed (R) states of HscA (*15*, *17*, *21*). Accordingly, the low level of

† This work was supported by a grant from the National Institutes of Health (GM62542 to M.K.J.)

* Corresponding author: telephone, 706-542-9378; fax, 706-542-2353; e-mail, johnson@chem.uga.edu.

[1] Abbreviations: CD, circular dichroism; DTT, dithiothreitol; Fdx, ferredoxin; Hsc, heat-shock cognate protein; ISC, iron−sulfur cluster biosynthesis machinery; SDS−PAGE, sodium dodecyl sulfate−polyacrylamide gel electrophoresis; SUF, sulfur mobilization iron−sulfur cluster biosynthesis machinery.

10.1021/bi061237w CCC: $33.50
Published on Web 08/25/2006

intrinsic ATPase activity exhibited by HscA is stimulated by interaction with HscB and greatly stimulated by a combination of HscB and IscU (*21*).

In spite of these major advances in understanding the biochemistry of HscA and HscB, there is currently no direct information concerning their specific function in the maturation of Fe-S proteins. Indeed, there are conflicting reports as to whether the role of the chaperone system is to facilitate the assembly of clusters on IscU (*25*) or the transfer of clusters preassembled on IscU to acceptor proteins (*26*). Immunoprecipitation studies in yeast indicated that functional depletion of the homologous Fe-S cluster assembly-associated chaperones resulted in increased accumulation of Fe on Isu (eukaryotic IscU), which suggested a role in mediating cluster transfer to acceptor proteins (*26*). In contrast, cluster transfer from *Thermotoga maritima* [2Fe-2S]IscU and human [2Fe-2S]Isu to apo human Fd was found to be inhibited by the nonspecific *T. maritima* DnaK/DnaJ chaperone system, irrespective of the presence or absence of nucleotides (*25*). Rather, on the basis of a modest increase in the stability of the [2Fe-2S] cluster-bound form of IscU in the presence of DnaK, the chaperone system was proposed to play a role in facilitating cluster assembly on IscU (*25*). In order to address the role of the ISC-specific HscA/HscB chaperone system in cluster assembly, we report here the results of EPR- and CD-monitored in vitro cluster transfer experiments between [2Fe-2S]IscU and apo-IscFdx using *Azotobacter vinelandii* Isc proteins. The results indicate that the HscA/HscB chaperone system greatly stimulates the rate of cluster transfer in an ATP-dependent process.

MATERIALS AND METHODS

All chemicals were purchased from Sigma-Aldrich or Fisher, unless otherwise stated. The *Escherichia coli* C41-[DE3] overexpression strain was provided by Professor John E. Walker (Medical Research Council, Cambridge, U.K.). The plasmids pDB1303 overexpressing *A. vinelandii* HscA and pDB1036 overexpressing *A. vinelandii* HscB were a kind gift from Professor Dennis Dean (Virginia Polytechnic Institute and State University). Anaerobic experiments were performed under Ar in a Vacuum Atmospheres glovebox at oxygen levels of <1 ppm. Protein concentrations were determined by the *DC* protein assay (Bio-Rad), using BSA as a standard. Iron concentrations were determined colorimetrically using bathophenanthroline under reducing conditions, after digestion of the protein in 0.8% $KMnO_4$/0.2 M HCl (*27*).

Preparation of A. vinelandii IscU and IscFdx Samples. *A. vinelandii* IscU containing 1.2 $[2Fe\text{-}2S]^{2+}$ clusters/dimer ($A_{456}/A_{280} = 0.31$) and holo *A. vinelandii* IscFdx (FdIV) (1.0 $[2Fe\text{-}2S]^{2+}$ cluster/monomer; $A_{458}/A_{280} = 0.51$) were prepared as previously described (*5*, *28*). The $[2Fe\text{-}2S]^{2+}$ cluster concentrations of the *A. vinelandii* IscU and IscFdx samples used in this work were based on experimentally determined extinction coefficients (as assessed by Fe and protein determinations) and are in excellent agreement with the published values [$\epsilon_{456} = 9.2\ mM^{-1}\ cm^{-1}$ for IscU (*5*) and $\epsilon_{458} = 7.1\ mM^{-1}\ cm^{-1}$ for IscFdx (*28*)]. Apo-IscFdx was prepared by acid precipitation of the holoprotein with trichloroacetic acid to a final concentration of 1.5%. The precipitate was centrifuged, and the resulting protein pellet was resolubilized inside the glovebox with 100 mM Tris-HCl, pH 7.5, anaerobic buffer containing 1 mM DTT. The apo-IscFdx was frozen and stored in liquid nitrogen.

Overexpression and Purification of A. vinelandii HscA and HscB. The *E. coli* C41[DE3]pDB1303 and C41[DE3]-pDB1036 strains were grown at 37 °C in terrific broth containing 100 μg/mL carbenicillin. When the cultures reached an OD_{600} between 0.9 and 1.2, isopropyl 1-thio-β-D-galactopyranoside (IPTG) was added to a final concentration of 0.8 mM, and the bacterial cultures were further cultivated at 28 °C for 20 h. The cells were harvested by centrifugation at 9000*g* for 5 min at 4 °C and stored at −80 °C until further use.

Cell paste (30 g) was thawed and resuspended in 90 mL of buffer A [100 mM Tris-HCl buffer, pH 7.5, containing 1 mM dithiothreitol (DTT)]. Phenylmethanesulfonyl fluoride (PMSF) (13 mg), 10 μg/mL DNase I (Roche), and 10 μg/mL RNase A (Roche) were added to the mixture. The cells were broken by intermittent sonication, and the cell debris was removed by centrifugation at 39700*g* for 1 h at 4 °C. The cell-free extract containing HscA or HscB was purified by anion-exchange chromatography with a 70 mL Q-Sepharose column. The protein was eluted with a 0.0−1.0 M NaCl gradient using 100 mM Tris-HCl buffer, pH 7.5, containing 1 mM dithiothreitol (DTT). The purest fractions, as judged by SDS−PAGE analysis, were pooled and dialyzed into 100 mM Tris-HCl, pH 7.5, containing 1 mM dithiothreitol (DTT) and 1.0 M ammonium sulfate by ultrafiltration using a YM30 (for HscA) or YM10 (for HscB) membrane. The protein was then further purified by binding to a 50 mL phenyl-Sepharose high-performance fast-flow column and eluting with a 1.0−0.0 M ammonium sulfate gradient using buffer A. Fractions containing HscA or HscB, as judged by SDS−PAGE analysis, were combined, dialyzed into buffer A by ultrafiltration using a YM30 or YM10 membrane, and purified using size exclusion chromatography (Superdex 200 for HscA or Superdex 75 for HscB). The purified proteins were exchanged into anaerobic buffer A inside the glovebox, concentrated to >50 mg/mL via ultrafiltration, and stored in liquid nitrogen until further use. The samples of *A. vinelandii* HscA and HscB used in this work were >95% pure as judged by SDS−PAGE analysis.

ATPase Activity Assays. The ATPase activity of HscA in the presence and absence of excess HscB and/or apo-IscU and in the cluster transfer reaction mixture was assessed at 23 °C by measuring the phosphate released via a coupled enzyme assay with the EnzChek phosphate assay kit (Invitrogen).

Cluster Transfer Experiments. The time course of cluster transfer from *A. vinelandii* [2Fe-2S]IscU to apo-IscFdx was monitored under anaerobic conditions at 23 °C using UV−visible CD and EPR spectroscopy. Reactions were carried in 100 mM Tris-HCl buffer, pH 7.5, containing 1 mM DTT, and the reaction mixtures (0.2 mL for CD and 1.3 mL for EPR) were 0.10 mM in apo-IscFdx (pretreated with 8 mM DTT for 45 min prior to use in cluster transfer experiments) and 0.30 mM in IscU monomer with 1.2 $[2Fe\text{-}2S]^{2+}$ clusters/IscU dimer to give a final IscU $[2Fe\text{-}2S]^{2+}$ cluster concentration of 0.18 mM. Reactions were also carried out in the presence of one or more (or all) of the following reagents: *A. vinelandii* HscA (final concentration 0.30 mM), *A. vinelandii* HscB (final concentration 0.30 mM), 2.0 mM

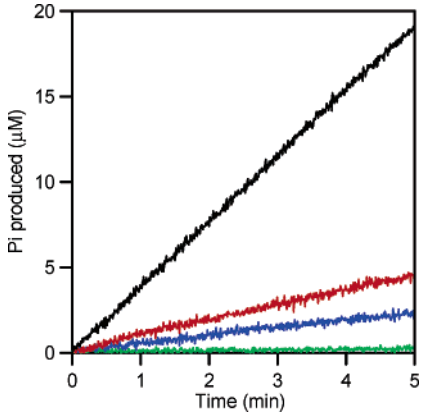

FIGURE 1: ATPase activity of *A. vinelandii* HscA. Time course of ATP hydrolysis at 23 °C by 1.0 μM HscA alone (green), in the presence of 100 μM *A. vinelandii* HscB (blue), in the presence of 100 μM *A. vinelandii* HscB and 100 μM *A. vinelandii* apo-IscU (red), and in the presence of 100 μM *A. vinelandii* HscB, 100 μM *A. vinelandii* apo-IscU, and 150 mM KCl (black).

ATP, 40 mM $MgCl_2$, and 150 mM KCl. The zero time point corresponds to the addition of ATP or the addition of [2Fe-2S]IscU for reaction mixtures not containing ATP. CD experiments were carried out in 0.1 cm cuvettes, and changes in the CD spectra at 505 nm were used to assess concentration of holo-IscFdx as a function of time (see Results for details). EPR experiments were carried out by withdrawing 240 μL aliquots of the reaction mixture at various time points, reducing anaerobically with 10 μL of 50 mM sodium dithionite (final concentration 2 mM), and freezing in liquid nitrogen within 20 s of reduction. X-band EPR spectra of the reaction mixture were recorded at 60 K with 0.1 mW microwave power and 0.63 G modulation amplitude, and the concentration of reduced holo-IscFdx was quantified by double integration of the $g = 2.02$, 1.94, and 1.93 resonance versus a 1 mM CuEDTA standard recorded under the same conditions. For both EPR and CD studies, the time course of holo-IscFdx formation was analyzed by fitting to second-order kinetics (initial concentration of IscU $[2Fe\text{-}2S]^{2+}$ clusters = 0.18 mM and apo-IscFdx = 0.10 mM) using the Chemical Kinetics Simulator software package (IBM).

Spectroscopic Measurements. UV−visible absorption and CD spectra were obtained using a Shimadzu UV-3101PC spectrophotometer and a Jasco J715 spectropolarimeter, respectively. Resonance Raman spectra were recorded at 17 K as previously described (*29*), and X-band EPR spectra were recorded using a Bruker ESP-300E spectrometer equipped with an Oxford Instrument ESR-9 flow cryostat.

RESULTS

HscA ATPase Activity. A. vinelandii HscA exhibits a low basal level of ATPase activity corresponding to 0.035 mol of ATP hydrolyzed (mol of HscA)$^{-1}$ min^{-1}. However, the ATPase activity was enhanced 13-fold in the presence of a 100-fold excess of HscB and 25-fold in the presence of a 100-fold excess of both HscB and apo-IscU; see Figure 1. These activities were measured in the absence of K^+ ions which are generally required for optimal ATPase activity of Hsp70 molecular chaperones (*30*). Hence the activities were repeated in the presence of 150 mM KCl, which approximates to the cytoplasmic concentration of K^+ ions (*30*). No significant change in activity was observed for HscA alone or in the presence of HscB (data not shown), but K^+ ions produced an additional 4-fold enhancement of the activity in the presence of HscB and apo-IscU; see Figure 1. Hence, in the presence of 150 mM KCl, the basal level ATPase activity of HscA was enhanced approximately 100-fold in the presence of a 100-fold excess of both HscB and apo-IscU. Such behavior is typical of Hsp70 chaperones, in general, and similar studies with *E. coli* Isc proteins reported a 400-fold increase in the ATPase activity of HscA in the presence of HscB and apo-IscU (*21*).

Spectroscopic Characterization of [2Fe-2S]IscU and IscFdx. The effect of addition of stoichiometric amounts of HscA, HscB, or HscA and HscB together, each in the absence or presence of a 10-fold excess of MgATP or MgADP, on the spectroscopic properties of [2Fe-2S]IscU and IscFdx was evaluated to assess the viability of spectroscopic approaches for monitoring chaperone binding to both proteins and cluster transfer from [2Fe-2S]IscU to apo-IscFdx. The $[2Fe\text{-}2S]^{2+,+}$ cluster environment in holo-IscFdx is not perturbed by the chaperone system, as evidenced by no changes in the UV−visible absorption/CD and resonance Raman spectra of oxidized IscFdx and the EPR spectrum of dithionite-reduced IscFdx [$g = 2.02$, 1.94, and 1.93 (*28*)] on stoichiometric addition of the chaperone system components (data not shown). The UV−visible absorption and CD spectra of the oxidized Fdx and the EPR spectrum of the reduced protein were in excellent agreement with the previously published data for *A. vinelandii* IscFdx (FdIV) (*28*).

A. vinelandii IscU is a dimeric protein as evidenced by gel filtration and chemical cross-linking studies (*31*). In accord with previous studies (*5*), the [2Fe-2S]IscU used in this work consistently contained 1.2 ± 0.1 $[2Fe\text{-}2S]^{2+}$ clusters per IscU dimer, and the cluster was rapidly degraded on dithionite reduction, without generating an EPR-detectable $S = {}^1/_2$ $[2Fe\text{-}2S]^+$ cluster. No significant changes in the UV−visible absorption or resonance Raman spectra of the $[2Fe\text{-}2S]^{2+}$ center (*5*) were apparent on stoichiometric addition of the chaperone components, individually or together, indicating no significant perturbation in the electronic or vibrational properties of the cluster. However, stoichiometric addition of chaperone components, individually or combined, does perturb the chirality of the cluster environment, as evidenced by significant changes in the relative intensities and energies of bands in the CD spectra; see Figure 2. Very similar changes were observed on addition of HscA, HscB, and HscA/HscB together (see Figure 2), and in each case, no further changes in the CD spectra were apparent on addition of a 7-fold excess of MgATP or MgADP or increasing the HscA/HscB to IscU stoichiometry from 1:1 to 3:1. The lability of the IscU $[2Fe\text{-}2S]^{2+}$ cluster in the absence and presence of the chaperone system components was assessed by monitoring the UV−visible absorption and CD spectra of [2Fe-2S]IscU at room temperature under strictly anaerobic conditions. No significant changes in either the form or intensity of the UV−visible absorption and CD spectra were observed over a period of 12 h for samples with and without the chaperone system components, both in the presence and in the absence of MgADP or MgATP. We conclude that both HscA and HscB interact with [2Fe-2S]IscU in a manner that leads to similar changes in the

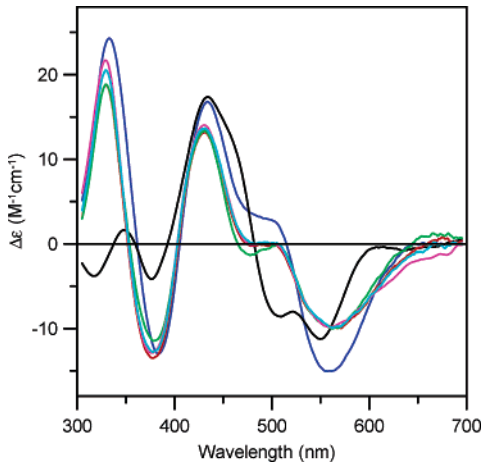

FIGURE 2: UV−visible CD spectra of *A. vinelandii* IscFdx (FdIV) (black) and *A. vinelandii* [2Fe-2S]IscU in the absence (blue) and presence of HscA (green), HscB (magenta), HscA/HscB (cyan), and HscA/HscB/MgATP (red). The IscFdx sample was 0.10 mM in both protein and $[2Fe\text{-}2S]^{2+}$ clusters (1.0 $[2Fe\text{-}2S]^{2+}$ cluster/monomer), and the [2Fe-2S]IscU samples were 0.30 mM in IscU monomer and 0.18 mM in $[2Fe\text{-}2S]^{2+}$ clusters (1.2 $[2Fe\text{-}2S]^{2+}$ clusters/IscU dimer). [2Fe-2S]IscU samples treated with HscA, HscB, HscA/HscB, and HscA/HscB/MgATP were 0.30 mM HscA and/or HscB, and the MgATP-containing sample was 2.0 mM ATP and 40 mM $MgCl_2$. $\Delta\epsilon$ values are based on the $[2Fe\text{-}2S]^{2+}$ cluster concentration, and the path length was 0.1 cm.

chirality of the $[2Fe\text{-}2S]^{2+}$ cluster environment. However, in the absence of an appropriate acceptor protein, neither HscA nor HscB nor HscA/HscB together increase the lability of the $[2Fe\text{-}2S]^{2+}$ centers on IscU, even in the presence of MgATP.

Kinetics of [2Fe-2S]IscU to Apo-IscFdx Cluster Transfer. Two viable spectroscopic approaches for direct monitoring of the time course of $[2Fe\text{-}2S]^{2+}$ cluster transfer from [2Fe-2S]IscU to apo-IscFdx are suggested by the spectroscopic results reported above. The first uses the observation that only holo-IscFdx exhibits an EPR signal on dithionite reduction and involves taking samples from the reaction mixture at various time periods, freezing in EPR tubes immediately after dithionite reduction, and quantifying the sharp, near-axial resonance from reduced holo-IscFdx (g = 2.02, 1.94, and 1.93). The second makes use of the differences in the CD spectra of [2Fe-2S]IscU and holo-IscFdx and involves monitoring changes in the CD spectrum of the reaction mixture as a function of time. Both approaches were used to monitor the kinetics of cluster transfer from [2Fe-2S]IscU to apo-IscFdx under the same experimental conditions in the presence and absence of components of the HscA/HscB chaperone system. The observed rate constants for cluster transfer using the EPR and CD experiments agreed within experimental error of the measurements (±15% for EPR studies and (±5% for CD studies). Only the results of the CD experiments are presented herein, as this approach provides more precise rate constants by facilitating continuous monitoring of both the [2Fe-2S]IscU and holo-IscFdx concentrations in the reaction mixture and avoiding reductive degradation of the cluster on [2Fe-2S]-IscU prior to assessing the holo-IscFdx concentration.

UV−visible CD spectra of cluster transfer reaction mixtures that were initially 0.18 mM in IscU $[2Fe\text{-}2S]^{2+}$ clusters and 0.10 mM in apo-IscFdx are shown in Figures 3 and 4. Spectra were recorded initially after 2 and 5 min of reaction and subsequently at 5 min intervals up to 120 min. As the CD spectrum of [2Fe-2S]IscU is perturbed by HscA/HscB binding (Figure 2), Figure 3 shows data in the absence of the chaperone system (Figure 3A) and Figure 4 shows data in the presence of stoichiometric HscA/HscB (Figure 4C), stoichiometric HscA/HscB plus 2 mM MgATP (Figure 4B), and stoichiometric HscA/HscB plus 2 mM MgATP and 150 mM KCl (Figure 4A). Simulated CD data, based on weighted

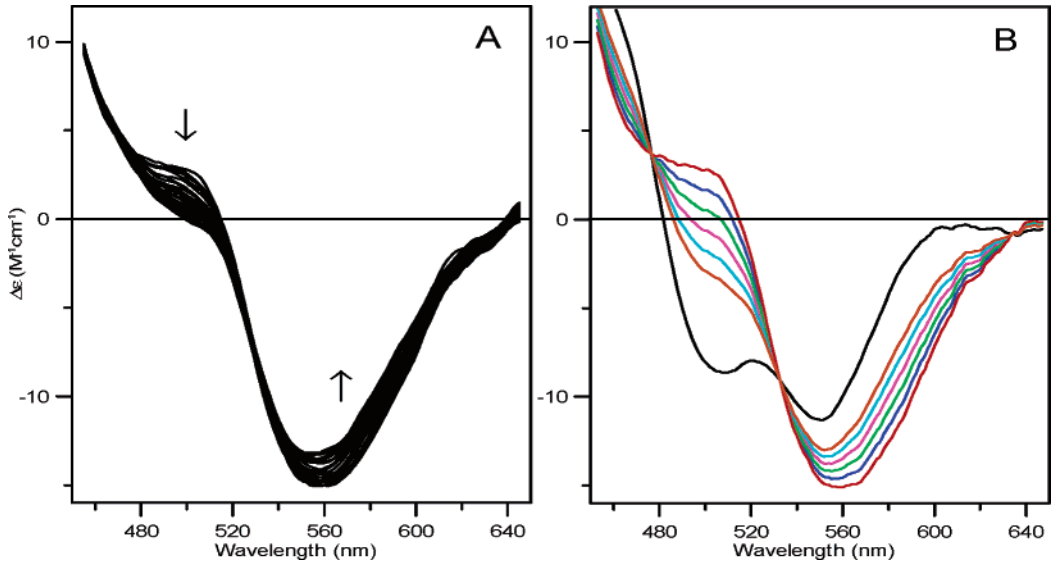

FIGURE 3: Time course of cluster transfer from *A. vinelandii* [2Fe-2S]IscU to apo-IscFdx monitored by UV−visible CD spectroscopy at 23 °C. (A) CD spectra recorded at 2, 5, 10, 15, 20, 25, 30, 35, 40, 45, 50, 55, 60, 65, 70, 75, 80, 85, 90, 95, 100, 105, 110, 115, and 120 min after adding [2Fe-2S]IscU (0.30 mM in IscU monomer with 1.2 $[2Fe\text{-}2S]^{2+}$ clusters/IscU dimer to give a final $[2Fe\text{-}2S]^{2+}$ cluster concentration of 0.18 mM) to apo-IscFdx (0.10 mM final concentration). The arrows indicate the change in CD intensity with increasing time. (B) Simulated CD spectra corresponding to quantitative $[2Fe\text{-}2S]^{2+}$ cluster transfer from [2Fe-2S]IscU to apo-IscFdx resulting in 20% (blue), 40% (green), 60% (magenta), 80% (cyan), and 100% (orange) reconstitution of holo-IscFdx for the reaction mixture used in (A). The simulated CD spectra were constructed from weighted averages of the spectra for [2Fe-2S]IscU (red) and holo IscFdx (black). $\Delta\epsilon$ values are based on the $[2Fe\text{-}2S]^{2+}$ cluster concentration, and the path length was 0.1 cm.

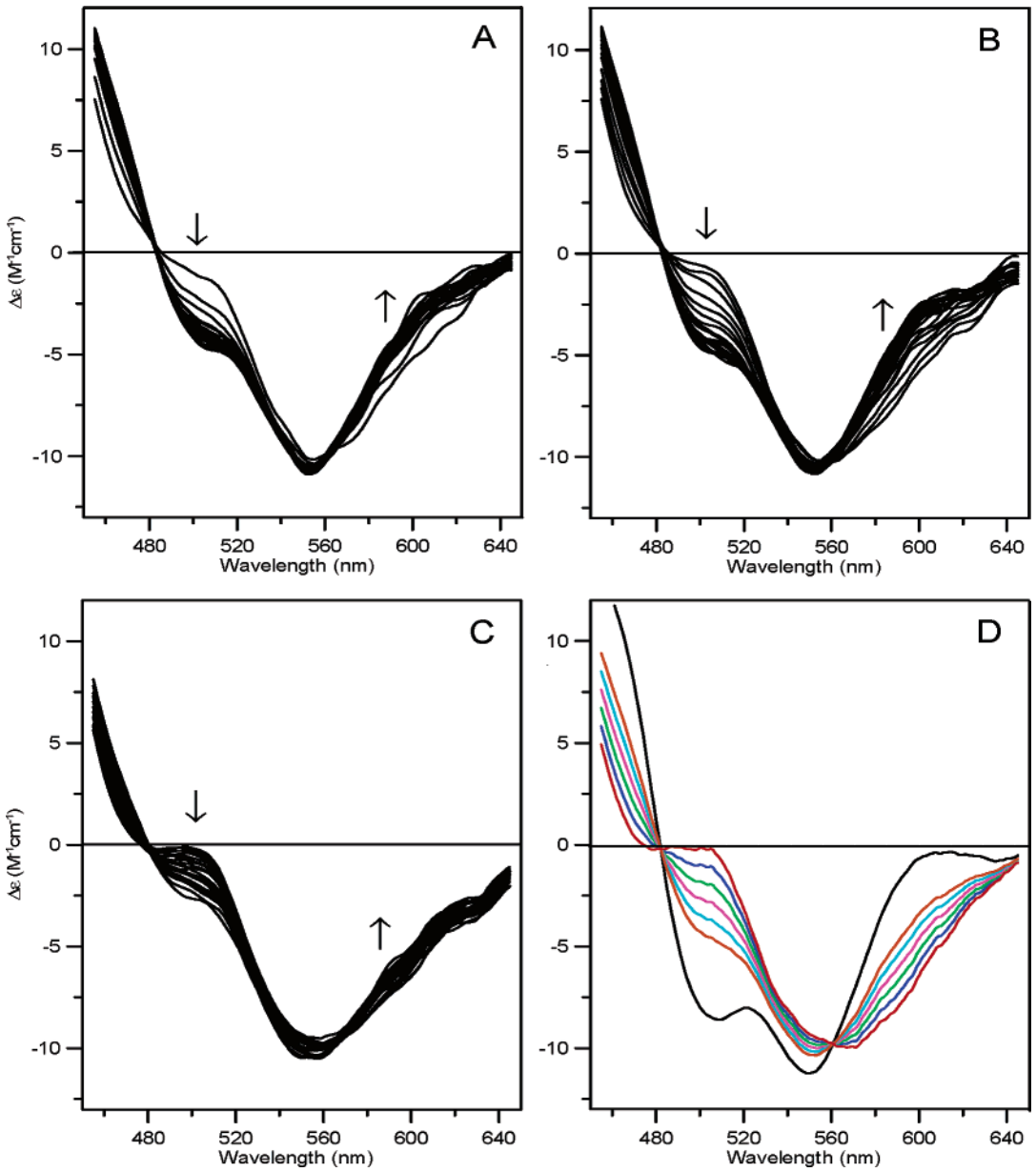

FIGURE 4: Time course of cluster transfer from *A. vinelandii* [2Fe-2S]IscU to apo-IscFdx in the presence of HscA, HscB, MgATP, and KCl monitored by UV−visible CD spectroscopy at 23 °C. Conditions are the same as described in Figure 3 except for the presence of 0.30 mM HscA, 0.30 mM HscB, 2.0 mM ATP, 40 mM $MgCl_2$, and 150 mM KCl (A), 0.30 mM HscA, 0.30 mM HscB, 2.0 mM ATP, and 40 mM $MgCl_2$ (B), and 0.30 mM HscA and 0.30 mM HscB (C). The arrows indicate the change in CD intensity with increasing time. (D) Simulated CD spectra corresponding to quantitative $[2Fe\text{-}2S]^{2+}$ cluster transfer from HscA/HscB-treated [2Fe-2S]IscU to apo-IscFdx resulting in 20% (blue), 40% (green), 60% (magenta), 80% (cyan), and 100% (orange) reconstitution of holo-IscFdx for the reaction mixtures used in (A), (B), and (C). The simulated CD spectra were constructed from weighted averages of the spectra for HscA/HscB/MgATP-treated [2Fe-2S]-IscU (red) and holo IscFdx (black). $\Delta\epsilon$ values are based on the $[2Fe\text{-}2S]^{2+}$ cluster concentration, and the path length was 0.1 cm.

averages of the CD spectra for [2Fe-2S]IscU or HscA/HscB-treated [2Fe-2S]IscU (red) and holo-IscFdx (black), corresponding to quantitative $[2Fe\text{-}2S]^{2+}$ cluster transfer from [2Fe-2S]IscU to apo-IscFdx resulting in 20%, 40%, 60%, 80%, and 100% reconstitution of holo-IscFdx are shown in Figures 3B and 4D, respectively. In all cases, the agreement between the experimental and simulated data is excellent, indicating $[2Fe\text{-}2S]^{2+}$ cluster transfer without any significant cluster degradation. Moreover, cursory inspection of the data clearly demonstrates that the rate of cluster transfer from [2Fe-2S]IscU to apo-IscFdx is not significantly enhanced by the addition of HscA/HscB alone, with both samples achieving ~50% reconstitution of holo-IscFdx after 120 min. In contrast, the rate of cluster transfer is dramatically enhanced by the presence of excess MgATP. Complete reconstitution of holo-IscFdx is achieved after 120 min, and the rate of cluster transfer is clearly further enhanced by the presence of 150 mM KCl (cf. Figure 4A,B).

Quantitative assessment of the rates of cluster transfer was obtained by monitoring CD changes at 505 nm, the wavelength associated with the maximum difference in CD intensity between [2Fe-2S]IscU and holo-IscFdx; see Figure 2. In the presence of the chaperone components, [2Fe-2S]-IscU has negligible CD intensity at 505 nm (see Figure 2), enabling direct assessment of the holo-IscFdx concentration as a function of time. In the absence of the chaperone system, holo-IscFdx concentrations as a function of time were assessed using a calibration curve constructed on the basis

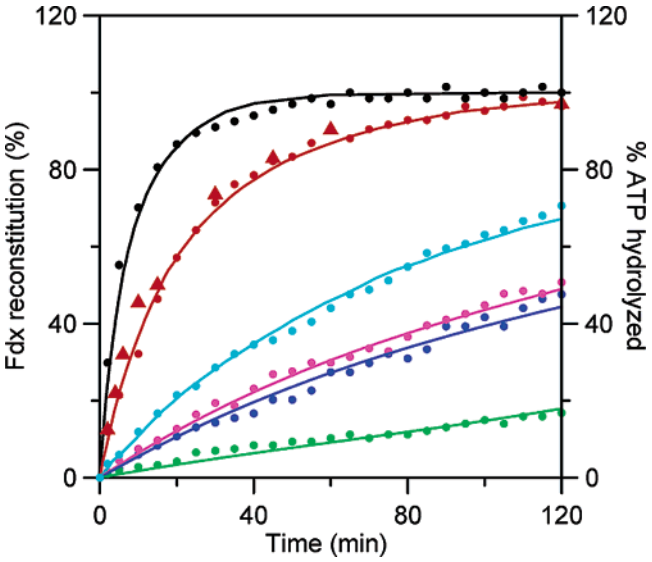

FIGURE 5: Kinetic analysis of [2Fe-2S]IscU-mediated reconstitution of apo-IscFdx monitored by CD spectroscopy. The conditions are described in Figures 3 and 4, and data points corresponding to the extent of IscFdx reconstitution as a function of time are shown as solid circles with solid lines corresponding to best fits to second-order kinetics with the initial concentration of [2Fe-2S] clusters on IscU = 0.18 mM and the initial concentration of apo-IscFdx = 0.10 mM. Black: [2Fe-2S]IscU-mediated reconstitution in the presence of HscA, HscB, MgATP, and KCl (rate constant = 800 M^{-1} min^{-1}). Red: [2Fe-2S]IscU-mediated reconstitution in the presence of HscA, HscB, and MgATP (rate constant = 280 M^{-1} min^{-1}). Cyan: [2Fe-2S]IscU-mediated reconstitution in the presence of HscA, HscB, and MgADP (rate constant = 65 M^{-1} min^{-1}). Blue: [2Fe-2S]IscU-mediated reconstitution in the presence of HscA and HscB (rate constant = 31 M^{-1} min^{-1}). Magenta: [2Fe-2S]IscU-mediated reconstitution (rate constant = 36 M^{-1} min^{-1}). Green: Anaerobic reconstitution of 0.10 mM apo-IscFdx using 0.36 mM Fe^{2+} and 0.36 mM S^{2-} (rate constant = 9 M^{-1} min^{-1}). The solid red triangles indicate the extent of ATP hydrolysis (right axis) during [2Fe-2S]IscU-mediated reconstitution of apo-IscFdx in the presence of HscA, HscB, and MgATP, as determined by phosphate assays of samples taken from the reaction mixture at selected time intervals.

of changes in the simulated data at 505 nm (see Figure 3B). Figure 5 shows results for reaction mixtures containing no chaperone components, HscA/HscB, HscA/HscB/MgADP, HscA/HscB/MgATP, and HscA/HscB/MgATP/KCl, along with parallel CD data for the time course of reconstitution of apo-IscFdx using $FeSO_4$ and Na_2S in amounts equivalent to the iron and sulfide content of the [2Fe-2S]IscU used in cluster transfer experiments. In all cases the data are well fit to second-order kinetics with the initial concentration of [2Fe-2S] clusters on IscU = 0.18 mM and the initial concentration of apo-IscFdx = 0.10 mM, and second-order rate constants for these reaction mixtures and for parallel reactions mixtures containing HscA and HscA/MgATP are graphically compared in Figure 6. The data show that the rate of IscFdx reconstitution is enhanced ~4-fold using [2Fe-2S]IscU compared to equivalent amounts of Fe^{2+} and S^{2-}. Taken together with the CD evidence for no significant $[2Fe-2S]^{2+}$ cluster degradation in the reaction mixture, this is consistent with intact cluster transfer from [2Fe-2S]IscU to apo-IscFdx. However, the rate of cluster transfer is not significantly enhanced by HscA alone, in the presence of MgATP, or in the presence of HscA/HscB without concurrent addition of MgADP or MgATP. In contrast, the rate of intact cluster transfer from HscA/HscB-treated [2Fe-2S]IscU is increased ~2-fold in the presence of MgADP and ~10-fold in the presence of excess MgATP. Morever, the reaction mixture containing MgATP exhibited a further ~3-fold rate enhancement on addition of 150 mM KCl. No rate enhancement was observed for the parallel MgADP sample. This result is consistent with rate simulation by an ATP-dependent reaction, as 150 mM KCl was found to induce a 4-fold increase in the ATPase activity of HscA in the presence of HscB and IscU; see Figure 1. In addition, phosphate assays of samples taken from the reaction mixture without KCl at selected time periods demonstrate that ATP hydrolysis is occurring concomitant with cluster transfer; see solid triangles in Figure 5. Unfortunately, the ATP requirement for cluster transfer cannot be reliably assessed from these data, because ATP hydrolysis by HscA, HscA/HscB, and HscA/HscB/IscU can occur without cluster transfer; see Figure 1. Nevertheless, the rate stimulation of cluster transfer in the presence of HscA/HscB/MgATP, coupled with the additional

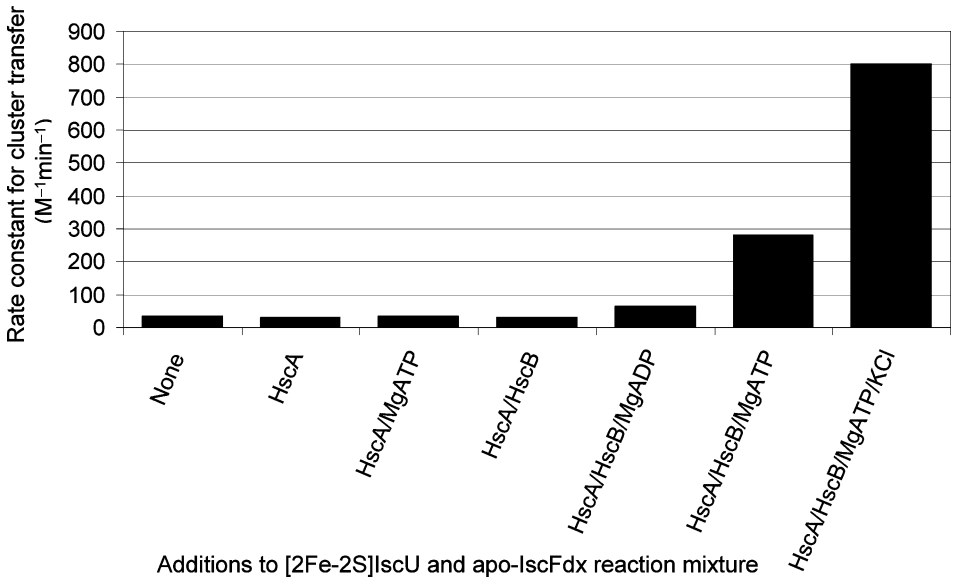

FIGURE 6: Summary of the effect of chaperone components on the rate of [2Fe-2S]IscU to apo-IscFdx cluster transfer. The conditions are described in Figures 3−5.

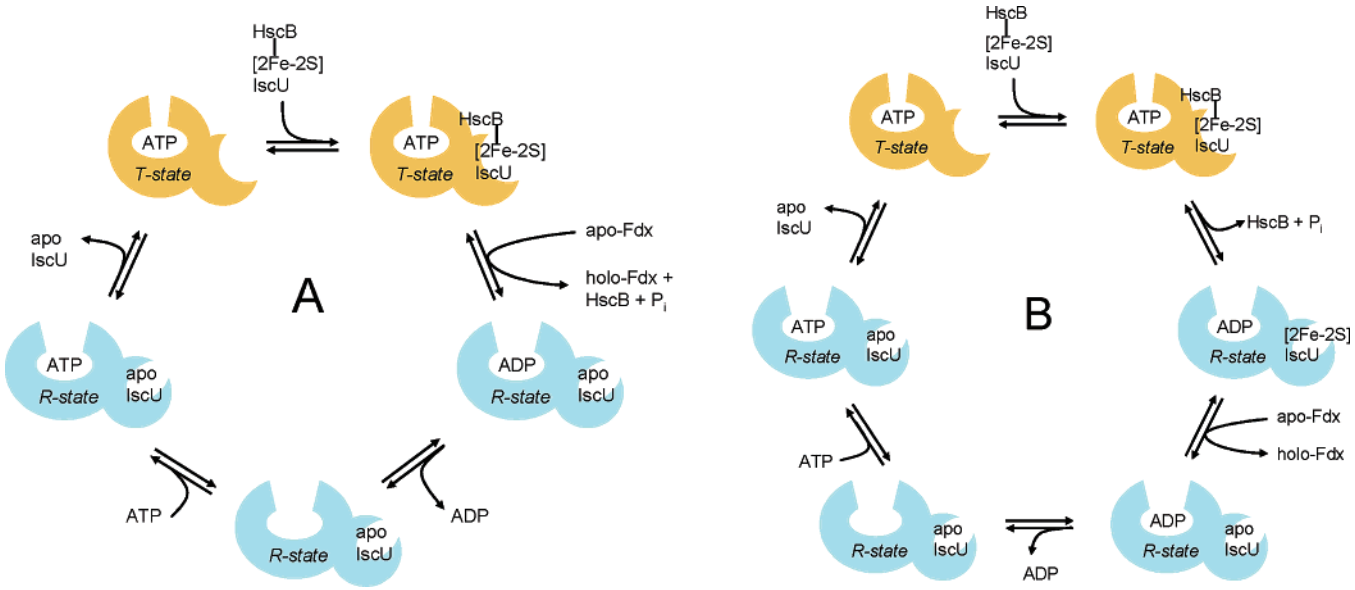

FIGURE 7: Possible mechanistic schemes for how the HscA/HscB/IscU chaperone cycle stimulates cluster transfer from [2Fe-2S]IscU to apo-IscFdx. The HscA chaperone cycle proposed by Silberg et al. (*17*) has been modified to incorporate the cluster transfer results reported in this work.

stimulation by KCl and the observation of concurrent ATP hydrolysis, makes a compelling case for HscA/HscB together enhancing the rate of [2Fe-2S] cluster transfer via an ATP-dependent reaction.

DISCUSSION

A plethora of genetic and biochemical studies have established that the HscA/HscB cochaperones and their eukaryotic homologues, Ssp1/Jac1, are essential for efficient maturation of Fe-S proteins using the ISC assembly machinery (*10*−*14*, *32*−*34*), but their specific role in the biogenesis of Fe-S clusters has remained elusive. In this work, we have presented direct, in vitro evidence that HscA/HscB facilitate [2Fe-2S] cluster transfer from the IscU scaffold protein to apo-IscFdx and provided the first evidence that cluster transfer involving IscU is an ATP-dependent process. Both results are in accord with in vivo and in vitro studies of the ISC assembly machinery in yeast mitochondria. In vivo evidence that Ssq1 and Jac1 are involved in a step after cluster assembly on the Isu1 scaffold protein was provided by ^{55}Fe immunoprecipation studies which revealed that Fe accumulation on Isu1 accompanies depletion of Ssq1 and Jac1 (*26*). Furthermore, recent in vitro studies indicated that Ssq1 and Jac1 are not important for Fe-S cluster synthesis on Isu1 (*35*). An ATP requirement for efficient assembly of Fe-S clusters was previously demonstrated by in vitro studies of detergent extracts from yeast mitochondria (*36*).

In contrast, the role demonstrated for HscA/HscB in this work is not in accord with a previous in vitro study of the effect of the homologous *T. maritima* DnaK/DnaJ chaperone system on cluster transfer from *T. maritima* [2Fe-2S]IscU and human [2Fe-2S]Isu to apo human Fdx (*25*). In this case cluster transfer was found to be inhibited by the nonspecific *T. maritima* DnaK/DnaJ chaperone system, irrespective of the presence or absence of nucleotides (*25*). Consequently, the chaperone system was proposed to play a role in facilitating cluster assembly on IscU, based on a modest increase in the stability of the [2Fe-2S] cluster-bound form of IscU in the presence of DnaK (*25*). However, our results clearly demonstrate that it is not appropriate to extrapolate results obtained with a nonspecific DnaK/DnaJ chaperone system in assessing the role of the ISC-specific HscA/HscB chaperone system. As discussed below, this assertion is further supported by several other lines of argument. The DnaK/DnaJ chaperone system facilitates protein folding, (dis)assembly, and transport and has broad substrate specificity (*18*), whereas HscA/HscB are specific for IscU, with HscA binding to the highly conserved LPPVK motif adjacent to the putative cluster binding site. Moreover, recent structural characterization of the HscA substrate-binding domain has shown that peptides bind with the opposite orientation to that observed in DnaK peptide complexes (*20*). *T. maritima* IscU is also unlikely to use a chaperone system to facilitate cluster transfer as it is part of a SUF (sulfur-mobilization) operon and is homologous with other SufU proteins (*1*). SUF operons do not encode homologues of the HscA/HscB molecular chaperones, and SufU proteins lack the signature LPPVK motif required for the interaction of IscU with HscA (*1*). Hence we conclude that the results of previous studies using SufU/IscU with the nonspecific DnaK/DnaJ chaperone system cannot be used to infer conclusions concerning the role of the HscA/HscB chaperone system in ISC-directed cluster assembly.

Current understanding of biochemical and structural properties of the ISC HscA/HscB molecular chaperone system is largely the result of the pioneering studies of Vickery and co-workers (*15*−*17*, *19*−*22*, *37*, *38*). This body of work has recently led to a detailed kinetic analysis of the regulation of the HscA ATPase reaction cycle by HscB and apo-IscU (*17*). ATP binding to HscA leads to a tense (T) state with decreased substrate-binding affinity. HscB binds and escorts IscU to HscA and enhances HscA binding of IscU in the ATP-bound T-state, leading to a transient HscA/ATP/HscB/IscU complex which undergoes ATP hydrolysis and loss of HscB to yield an ADP-bound relaxed (R) state with increased affinity for IscU. The IscU substrate is subsequently released after ADP/ATP exchange and the

R → T transition that occurs following ATP binding to HscA. Kinetic studies in the presence of saturating amounts of HscB and apo-IscU indicated that ATP hydrolysis and T → R conversion constitute the rate-determining step in the steady-state reaction cycle. As discussed below, the results presented here are consistent with this overall scheme and suggest two plausible mechanisms for coupling of the HscA ATPase cycle with cluster transfer from [2Fe-2S]IscU to apo-IscFdx; see Figure 7.

Our results demonstrate a crucial role for HscB in mediating ATP-dependent cluster transfer by HscA. CD data clearly demonstrate interaction between HscB and [2Fe-2S]-IscU, and kinetic data indicate that the presence of HscB in the reaction mixture is essential for optimal ATP-dependent HscA-mediated cluster transfer. Interestingly, on the basis of changes in the CD spectra of the [2Fe-2S] chromophore, it is likely that both HscB and HscA interact with [2Fe-2S]-IscU in a similar way with respect to the cluster environment. Overall, the in vitro cluster transfer data are in accord with the proposed role of HscB in delivering IscU to HscA and stimulating the ATPase activity of the resulting HscA/ATP/HscB/IscU ternary complex (*17*). Moreover, surface plasmon resonance measurements indicate that HscB interacts only with the ATP complex of HscA, indicating a specific role in recruiting IscU to the low substrate affinity T-state of HscA, and that HscB dissociates following ATP hydrolysis (*17*); see Figure 7.

The rate stimulation of cluster transfer in the presence of HscA/HscB/MgATP, coupled with the additional stimulation by KCl and evidence for concurrent phosphate production, indicates that the rate of [2Fe-2S] cluster transfer from IscU to apo-Fdx is kinetically dependent on ATP hydrolysis. Taken together with the evidence for high-affinity binding of IscU to the R-state HscA/ADP complex (*17*) and the observation that ADP binding to the R-state HscA/IscU complex does result in a modest (~2-fold) increase in the rate of the cluster transfer leads us to propose two possibilities for the interaction with apo-Fdx and the mechanism of ATP-dependent cluster transfer; see Figure 7. The first involves direct coupling between ATP hydrolysis and cluster transfer and requires interaction between apo-Fdx and the T-state HscA/ATP/HscB/IscU ternary complex. In this model, ATP hydrolysis and the concurrent T → R HscA conversion result in a conformational change in bound [2Fe-2S]IscU that facilitates cluster transfer to an acceptor protein and release of HscB; see Figure 7A. The second involves ATP hydrolysis preceding cluster transfer and involves interaction between apo-Fdx and the R-state HscA/ADP/IscU complex; see Figure 7B. In this model, cluster transfer is kinetically dependent on ATP hydrolysis or dependent on ATP for efficient interaction with HscB and therefore dependent on hydrolysis to reach the ADP state. The modest enhancement of the rate of cluster transfer on addition of ADP to the R-state HscA/[2Fe-2S]IscU complex is readily rationalized in terms of slower formation and recycling of the HscA/[2Fe-2S]IscU complex in the presence of ADP. The current data do not permit discrimination between these two alternative mechanistic proposals. Studies to address the detailed molecular mechanism of chaperone-assisted cluster transfer and to assess if chaperone-facilitated cluster transfer also occurs with [4Fe-4S]IscU are currently in progress.

ACKNOWLEDGMENT

We thank Professor Dennis R. Dean for providing plasmids for overexpressing *A. vinelandii* HscA, HscB, IscS, IscU, and IscFdx and for many insightful discussions. We are indebted to a reviewer for suggesting an alternative mechanistic proposal.

REFERENCES

1. Johnson, D., Dean, D. R., Smith, A. D., and Johnson, M. K. (2005) Structure, function and formation of biological iron-sulfur clusters, *Annu. Rev. Biochem. 74*, 247−281.
2. Lill, R., and Mühlenhoff, U. (2005) Iron-sulfur-protein biogenesis in eukaryotes, *Trends Biochem. Sci. 30*, 133−141.
3. Zheng, L., White, R. H., Cash, V. L., Jack, R. F., and Dean, D. R. (1993) Cysteine desulfurase activity indicates a role for NIFS in metallocluster biosynthesis, *Proc. Natl. Acad. Sci. U.S.A. 90*, 2754−2758.
4. Mihara, H., and Esaki, N. (2002) Bacterial cysteine desulfurases: their function and mechanisms, *Appl. Microbiol. Biotechnol. 60*, 12−23.
5. Agar, J. N., Krebs, B., Frazzon, J., Huynh, B. H., Dean, D. R., and Johnson, M. K. (2000) IscU as a scaffold for iron-sulfur cluster biosynthesis: Sequential assembly of [2Fe-2S] and [4Fe-4S] clusters in IscU, *Biochemistry 39*, 7856−7862.
6. Ollagnier-de-Choudens, S., Mattioli, T., Takahashi, Y., and Fontecave, M. (2001) Iron-sulfur cluster assembly. Characterization of IscA and evidence for a specific functional complex with ferredoxin, *J. Biol. Chem. 276*, 22604−22607.
7. Krebs, C., Agar, J. N., Smith, A. D., Frazzon, J., Dean, D. R., Huynh, B. H., and Johnson, M. K. (2001) IscA, an alternative scaffold for Fe-S cluster biosynthesis, *Biochemistry 40*, 14069−14080.
8. Ding, H., Harrison, K., and Lu, J. (2005) Thioredoxin reductase system mediates iron binding in IscA and iron-delivery for the iron-sulfur cluster assembly in IscU, *J. Biol. Chem. 280*, 30432−30437.
9. Chandramouli, K., Unciuleac, M.-C., Naik, S., Dean, D. R., Huynh, B. H., and Johnson, M. K. (2006) Formation and properties of [4Fe-4S] clusters on the IscU scaffold protein, *J. Biol. Chem.* (submitted for publication).
10. Takahashi, Y., and Nakamura, M. (1999) Functional assignment of the ORF2-*iscS*-*iscA*-*hscB*-*hscA*-*fdx*-ORF3 gene cluster involved in the assembly of Fe-S clusters in *Escherichia coli*, *J. Biochem. 126*, 917−926.
11. Tokumoto, U., and Takahashi, Y. (2001) Genetic analysis of the *isc* operon in *Escherichia coli* involved with the biogenesis of cellular iron-sulfur proteins, *J. Biochem. 130*, 63−71.
12. Voisine, C., Cheng, Y. C., Ohlson, M., Schilke, B., Hoff, K., Beinert, H., Marszalek, J., and Craig, E. A. (2001) Jac1, a mitochondrial J-type chaperone, is involved in the biogenesis of Fe/S clusters in *Saccharomyces cerevisiae*, *Proc. Natl. Acad. Sci. U.S.A. 98*, 1483−1488.
13. Lutz, T., Westermann, B., Neupert, W., and Herrmann, J. M. (2001) The mitochondrial proteins Ssq1 and Jac1 are required for the assembly of iron-sulfur clusters in mitochondria, *J. Mol. Biol. 307*, 815−825.
14. Kim, R., Saxena, S., Gordon, D. M., Pain, D., and Dancis, A. (2001) J-domain protein, Jac1p, of yeast mitochondria required for iron homeostasis and activity of Fe-S cluster proteins, *J. Biol. Chem. 276*, 17524−17532.
15. Silberg, J. J., Hoff, K. G., Tapley, T. L., and Vickery, L. E. (2001) The Fe/S assembly protein IscU behaves as a substrate for the molecular chaperone Hsc66 from *Escherichia coli*, *J. Biol. Chem. 276*, 1696−1700.
16. Hoff, K. G., Ta, D. T., Tapley, T. L., Silberg, J. J., and Vickery, L. E. (2002) Hsc66 substrate specificity is directed toward a discrete region of the iron-sulfur cluster template protein IscU, *J. Biol. Chem. 277*, 27353−27359.
17. Silberg, J. J., Tapley, T. L., Hoff, K. G., and Vickery, L. E. (2004) Regulation of the HscA ATPase reaction cycle by the co-chaperone HscB and the iron-sulfur cluster assembly protein IscU, *J. Biol. Chem. 279*, 53924−53931.
18. Mayer, M. P., Brehmer, D., Gassler, C. S., and Bukau, B. (2001) Hsp70 chaperone machines, *Adv. Protein Chem. 59*, 1−44.

19. Silberg, J. J., and Vickery, L. E. (2000) Kinetic characterization of the ATPase cycle of the molecular chaperone Hsc66 from *Escherichia coli*, *J. Biol. Chem. 275*, 7779−7786.
20. Cupp-Vickery, J. R., Peterson, J. C., Ta, D. T., and Vickery, L. E. (2004) Crystal structure of the molecular chaperone HscA substrate binding domain complexed with the IscU recognition peptide ELPPVKIHC, *J. Mol. Biol. 342*, 1265−1278.
21. Hoff, K. G., Silberg, J. J., and Vickery, L. E. (2000) Interaction of the iron-sulfur cluster assembly protein IscU with the Hsc66/Hsc20 molecular chaperone system of *Escherichia coli*, *Proc. Natl. Acad. Sci. U.S.A. 97*, 7790−7795.
22. Hoff, K. G., Cupp-Vickery, J. R., and Vickery, L. E. (2003) Contributions of the LPPVK motif of the iron-sulfur template protein IscU to interactions with the Hsc66-Hsc20 chaperone system, *J. Biol. Chem. 278*, 37582−37589.
23. Ramelot, T. A., Cort, J. R., Goldsmith-Fischman, S., Kornhaber, G. J., Xiao, R., Shastry, R., Acton, T. B., Honig, B., Montelione, G. T., and Kennedy, M. A. (2004) Solution NMR structure of the iron-sulfur cluster assembly protein U (IscU) with zinc bound at the active site, *J. Mol. Biol. 344*, 567−583.
24. Liu, J., Oganesyan, N., Shin, D. H., Jancarik, J., Yokota, H., Kim, R., and Kim, S.-H. (2005) Structural characterization of an iron-sulfur cluster assembly protein IscU in a zinc-bound form, *Proteins: Struct., Funct., Bioinf. 59*, 875−881.
25. Wu, S.-P., Mansy, S. S., and Cowan, J. A. (2005) Iron-sulfur cluster biosynthesis. Molecular chaperone DnaK promotes IscU-bound [2Fe-2S] cluster stability amd inhibits cluster transfer activity, *Biochemistry 44*, 4284−4293.
26. Mühlenhoff, U., Gerber, J., Richhardt, N., and Lill, R. (2003) Components involved in assembly and dislocation of iron-sulfur clusters on the scaffold protein Iscu1p, *EMBO J. 22*, 4815−4825.
27. Fish, W. W. (1988) Rapid colorimetric micromethod for the quantitation of complexed iron in biological samples, *Methods Enzymol. 158*, 357−364.
28. Jung, Y.-S., Gao-Sheridan, H. S., Christiansen, J., Dean, D. R., and Burgess, B. K. (1999) Purification and biophysical characterization of a new [2Fe-2S] ferredoxin from *Azotobacter vinelandii*, a putative [Fe-S] cluster assembly/repair protein, *J. Biol. Chem. 274*, 32402−32410.
29. Cosper, M. M., Krebs, B., Hernandez, H., Jameson, G., Eidsness, M. K., Huynh, B. H., and Johnson, M. K. (2004) Characterization of the cofactor content of *Escherichia coli* biotin synthase, *Biochemistry 43*, 2007−2021.
30. O'Brien, M. C., and McKay, D. B. (1995) How potassium affects the activity of the molecular chaperone Hsc70. I. Potassium is required for optimal ATPase activity, *J. Biol. Chem. 270*, 2247−2250.
31. Agar, J. N., Zheng, L., Cash, V. L., Dean, D. R., and Johnson, M. K. (2000) Role of the IscU protein in iron-sulfur cluster biosynthesis: IscS-mediated assembly of a $[Fe_2S_2]$ cluster in IscU, *J. Am. Chem. Soc. 122*, 2136−2137.
32. Dutkiewicz, R., Schilke, B., Knieszner, H., Walter, W., Craig, E. A., and Marszalak, J. (2003) Ssq1, a mitochondrial Hsp70 involved in iron-sulfur (Fe/S) center biogenesis. Similiarities to and differences from its bacterial counterpart, *J. Biol. Chem. 278*, 29719−29727.
33. Dutkiewicz, R., Schilke, B., Cheng, S., Knieszner, H., Craig, E. A., and Marszalek, J. (2004) Sequence-specific interaction between mitochondrial Fe-S scaffold protein Isu and Hsp70 Ssq1 is essential for their *in vivo* function, *J. Biol. Chem. 279*, 29167−29174.
34. Tokumoto, U., Nomura, S., Minami, Y., Mihara, H., Kato, S., Kurihara, T., Esaki, N., Kanazawa, H., Matsubara, H., and Takahashi, Y. (2002) Network of protein-protein interactions among iron-sulfur cluster assembly proteins in *Escherichia coli*, *J. Biochem. 131*, 713−719.
35. Dutkiewicz, R., Marszalek, J., Schilke, B., Craig, E. A., Lill, R., and Mühlenhoff, U. (2006) The Hsp70 chaperone Ssq1p is dispensable for iron-sulfur cluster formation on the scaffold protein Isu1p, *J. Biol. Chem. 281*, 7801−7808.
36. Mühlenhoff, U., Richhardt, N., Gerber, J., and Lill, R. (2002) Characterization of iron-sulfur protein assembly in isolated mitochondria. A requireiment for ATP, NADH, and reduced iron, *J. Biol. Chem. 277*, 29810−29816.
37. Tapley, T. L., and Vickery, L. E. (2004) Preferential substrate binding orientation by the molecular chaperone HscA, *J. Biol. Chem. 279*, 28435−28442.
38. Aoto, P. C., Ta, D. T., Cupp-Vickery, J. R., and Vickery, L. E. (2005) X-ray diffraction analysis of a crystal of HscA from *Escherichia coli*, *Acta Crystallogr. F61*, 715−717.

BI061237W